

ESD ACCESSION LIST

DRI Call No. 87460

Copy No. 1 of 2 cys.

Project Report

ETS-14

E. W. Rork

Night-Sky Astronomical Conditions
at the GEODSS ETS
from August 1975 to March 1977

21 June 1977

Prepared for the Department of the Air Force
under Electronic Systems Division Contract F19628-76-C-0002 by

Lincoln Laboratory

MASSACHUSETTS INSTITUTE OF TECHNOLOGY

LEXINGTON, MASSACHUSETTS



Approved for public release; distribution unlimited.

ADA043631

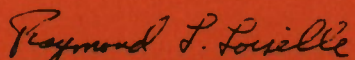
The work reported in this document was performed at Lincoln Laboratory, a center for research operated by Massachusetts Institute of Technology, with the support of the Department of the Air Force under Contract F19628-76-C-0002.

This report may be reproduced to satisfy needs of U.S. Government agencies.

The views and conclusions contained in this document are those of the contractor and should not be interpreted as necessarily representing the official policies, either expressed or implied, of the United States Government.

This technical report has been reviewed and is approved for publication.

FOR THE COMMANDER


Raymond L. Loiselle, Lt. Col., USAF
Chief, ESD Lincoln Laboratory Project Office

MASSACHUSETTS INSTITUTE OF TECHNOLOGY
LINCOLN LABORATORY

NIGHT-SKY ASTRONOMICAL CONDITIONS
AT THE GEODSS ETS FROM AUGUST 1975 TO MARCH 1977

E. W. RORK
Group 94

PROJECT REPORT ETS-14

21 JUNE 1977

Approved for public release; distribution unlimited.

LEXINGTON

MASSACHUSETTS

I. Introduction

Night-sky brightness, atmospheric extinction, image stability, and cloud cover have been monitored at the GEODSS Experimental Test System, located on the White Sands Missile Range, New Mexico, since August 1975. These quantities have been monitored because the ability of an electro-optical sensor, particularly one which is photon-noise limited, to detect a satellite is a function of them. The results of the measurements of these quantities up through March 1977, are tabulated in this note, accompanied by an explanation of their meaning, and the measurement techniques used.

II. Basis for the Measurements

1. Night-Sky Brightness. A satellite is detected if reflected sunlight from it produces an adequate signal-to-noise ratio (SNR) in a video field. Then, the brightness of a satellite required to produce this SNR is a function of the background noise from the surrounding night-sky brightness. The effect of night-sky brightness on the detection of faint astronomical sources is discussed quantitatively by Baum,¹ and his theory has been applied to the satellite detection problem by Weber and Brooks.² A result is, that for maximum detectability, the night-sky brightness near a satellite should be as low as possible. Thus, a survey of prevailing sky brightnesses at the GEODSS Experimental Test System is required in evaluating and predicting the performance of an electro-optical satellite detection system.

The units in which night-sky brightness is expressed are apparent visual magnitudes per square arc second, which mean the apparent visual magnitude of a single G-type star which, with no intervening atmosphere, produces the same photocurrent as a square arc second of sky. These units can be converted easily to a photon flux density at a telescope, or photoelectron flux density at an S-40 or S-25 photoemissive surface.³

The principal sources of night-sky brightness are scattered light from the moon and local sources of artificial light. The presence of aerosols, which scatter light, make the effects of these sources materially worse. Other natural sources of night-sky brightness include air glow from upper atmospheric chemical reactions, unresolved stars, the zodiacal light from sunlight scattered from interplanetary dust, and auroral emissions (chiefly for high latitude sites).

2. Atmospheric Extinction. A fraction of the reflected sunlight from satellites is scattered by the atmosphere, which causes a decrease in the ability of an E-O system to detect them. The prevailing atmospheric extinction is particularly important for the detection of satellites at low elevation angles, since reflected light from them passes through a greater portion of the earth's atmosphere, and the amount of light lost is proportionally greater. We define the atmospheric extinction coefficient at the number of visual magnitudes of light lost in passing through one atmospheric air mass; i.e., the light lost from a source at the observer's zenith. Since atmospheric extinction is a factor in the ability of a system to detect a satellite, a survey of atmospheric extinction properties at the GEODSS Experimental Test System is required.

The principal atmospheric condition causing a high extinction of light energy is the presence of aerosols, which may be moisture, clouds, local dust, or smoke.

3. Image Stability. The resolution of current GEODSS sensors is limited by the TV cameras to about 4 arc seconds. Hence, image stability requirements for a GEODSS site are considerably less than for a typical astronomical observatory where frequent 2-3 arc second stability would be undesirable. Since a few instances have occurred at the ETS when operations have been hindered because point image diameter was in excess of 4 arc seconds, i.e., noticeable on the video displays, occasional measurements of image stability have been made at the ETS. In addition, such measurements would be useful in evaluating future GEODSS sensors with higher resolution capabilities.

4. Weather and Cloud Conditions. It is of interest to the GEODSS program to know the number of nights during the year that the ETS would have operations hindered or cancelled by local weather and cloud conditions. Thus, since August 1975, local weather and cloud conditions at the ETS have been recorded on a daily basis. When nobody has been present at the ETS, such as on weekends and holidays, weather and cloud conditions have been recorded over Socorro, New Mexico, which is about 22 miles from the ETS.

III. Principle of the Measurements

1. Photoelectric Photometer for Extinction and Night-Sky Brightness

Measurements. A photoelectric photometer was used at the ETS to measure night-sky brightness and atmospheric extinction. The principle of its construction and operation is shown in Figure 1. It consists of:

- 1.1. an objective lens to collect the light;
- 1.2. a field stop diaphragm in the focal plane of the objective lens to determine the area of sky coverage;
- 1.3. a Fabry lens to place an image of the entrance pupil at the photocathode of the photomultiplier tube; and
- 1.4. a photomultiplier tube and associated electronics to record the light intensity.

The Fabry lens is necessary to ensure that the distribution of light across the photocathode remains independent of the position of a point image in the field stop.

The light intensity may be read directly from a strip chart recorder, and may also be recorded in digital form in the present computers for planned real-time extinction determinations.

Table 1 lists the characteristics of the two photometers at the ETS used to make the measurements.

The older photometer, which was obtained from the U.S.A.F. Avionics Laboratory, was a prototype exposure meter for the Baker-Nunn Cameras, and is described by Mackik and Kissell.⁴ In August 1976, the newer photometer was

put into operation at the ETS which had the advantages of greater aperture a narrower FOV, and a photomultiplier tube employing an S-20 photocathode, the same type used in the GEODSS TV cameras. In addition, the photomultiplier tube in the newer photometer was considerably less noisy than that of the older one, making accurate measurements easier to achieve. The spectral responses of the two photocathodes are shown in Figure 2, which were taken from an RCA manual.⁵ We observe that the wave length extent of responses of the two photocathodes is nearly the same, and that the wave length centroid of response for the RCA 111 photocathode is about $0.05\mu\text{m}$ longer than that of the S-20 photocathode. However, the sky brightness and extinction measurements taken with both photometers were identical within the error of measurement.

2. Calibration Procedures and Atmospheric Extinction Determination.

The photometer is calibrated by taking photometric readings of stars with temperatures similar to that of the sun, since we are interested in detecting satellite from reflected sunlight. The calibration stars chosen were of the 2nd or 3rd visual magnitude in brightness for the older photometer, and of the 5th or 6th visual magnitude for the new photometer. All stars were of the G-type spectral class with (B-V) magnitudes of $+0.5^{\text{m}}$ to 0.5^{m} , and were selected from the Arizona Tonantzintla Photometric Catalogue.⁶

The photometer produces a separate, measurable deflection due to dark current, night-sky brightness, and a calibration star when its image is placed in the field stop. We define:

x_d = deflection due to dark current,

x_b = deflection due to sky brightness,

x_s = deflection due to calibration star,

x_0 = deflection due to a 0 visual magnitude, G-type star when observed outside the earth's atmosphere,

m_s = catalogue visual magnitude of calibration star,

z_s = zenith distance of star producing photometer deflection x_s , and

ϵ = atmospheric extinction coefficient in visual magnitudes per air mass. Figure 3 illustrates the photometer deflections x_d , x_b , and x_s , as they would be measured from a strip chart record. Figure 4 is a reproduction of a photometric measurement of a calibration star illustrating x_b and x_s .

The number of atmospheric air masses through which light from a star passes may be expressed by the term $\sec(z_s)$. This "flat earth" approximation is shown by Hardie⁷ to be accurate to 2% at a zenith distance of 79° , which is suitable for our purpose.

Then, since the photometers used are linear devices, by the definition of a visual magnitude, we may write the following expression for x_s :

$$x_s = \frac{x_0}{(2.512)^{(m_s + \epsilon \sec z_s)}}. \quad (1)$$

Equation (1) may be put into a linear form as follows:

Transposing,

$$(2.512)^{(m_s + \epsilon \sec z_s)} = \frac{x_0}{x_s};$$

taking logarithms,

$$0.4(m_s + \epsilon \sec z_s) = \log x_0 - \log x_s; \quad (2)$$

transposing again,

$$(m_s + 2.5 \log x_s) = 2.5 \log x_0 - \epsilon(\sec z_s). \quad (3)$$

This equation is of the form

$$y = a_0 + a_1 x \quad (4)$$

where

$a_0 + 2.5 \log x_0$, the gain term of the photometer,

and

$a_1 = -\epsilon$, the atmospheric extinction term.

Then, if one measures x_s and z_s for each of several G-type stars at small and large zenith distances, a straight line may be fitted to (3) in the form (4) by a method such as that of least squares to determine a_0 and a_1 . A special computer program to perform this function is in operation on the computers at the GEODSS ETS, which is described in Section II, 4.

The atmospheric extinction coefficient determined in this way is an average value calculated from photometric deflections of the calibration stars, which are at different locations in the sky. Such a procedure presupposes that the atmospheric extinction coefficient is the same for all of the sky used for the measurements. Consequently, the sky must be visually inspected for the presence of clouds near the calibration stars before the extinction measurements are made. As a check to see if any clouds were partially obscuring a calibration star, the quantities $(m_s + 2.5 \log x_s)$ and $(\sec z_s)$ from equation 3 are plotted to see if:

2.1. The plot could be fitted by a straight line, and

2.2. if any photometric deflections caused the term $(m_s + 2.5 \log x_s)$ to lie far from the line.

In the event of a partial cloud cover, the brightness of a satellite in visual magnitudes is determined by comparing its photometric signal from the television sensor with that from the closest calibration star or stars to the satellite which are not obscured by the clouds. If a calibration star is

near the satellite at the same elevation as the satellite, atmospheric extinction is corrected for in determining the visual magnitude of the satellite, since the satellite reflections and star light are subject to the same extinction.

3. Night-Sky Brightness Determination. As stated in II, the night-sky brightness is expressed as the apparent visual magnitude of a single G-type star, as observed outside the atmosphere, which produces the same photocurrent as a square arc second of sky. If the sky of area A in square arc seconds (the FOV of the photometer) produces a deflection of x_b (Figure 3), then the deflection produced by one square arc sec is $\frac{x_b}{A}$. From equation (2), the extinction-corrected visual magnitude of a star which produces this deflection is:

$$\begin{aligned} m_b &= (m_s + \epsilon \sec z_s) = 2.5(\log x_0 - \log (\frac{x_b}{A})), \\ &= a_0 - 2.5 \log (\frac{x_b}{A}), \end{aligned}$$

which is the sky brightness in visual magnitudes per square arc second. The term a_0 was determined from the least squares analysis in the extinction calculation.

4. Operation of the Computer Program for the Atmospheric Extinction and Night-Sky Brightness Determination. A computer program has been written by A. S. Friedman and W. J. Taylor of Group 94, M.I.T., Lincoln Laboratory, to perform the least squares analysis to determine the atmospheric extinction coefficient and the night-sky brightness from the photometric data. The program is designated "PHM" in the LMT file on the computers at the ETS. The program requires as its input data:

4.1. Catalogue Visual Magnitude of Calibration Star.

4.2. Photometric Deflections due to Calibration Stars, Arbitrary Units.

4.3. Zenith Distances of Calibration Stars in Degrees.

4.4. The Area of Sky covered by the Photometer in Square Arc Seconds.

4.5. Photometer Deflections due to Sky Brightness, in the Same Units as the Calibration Star Deflections.

An example of the operation of the program is presented in the next section.

5. An Example of Atmospheric Extinction and Night-Sky Brightness Determination. As an illustration of the procedures just stated to determine the atmospheric extinction coefficient and night-sky brightness, Figure 5 is a reproduction of calibration star and sky brightness photometric deflections taken on the evening of Sept. 20, 1976. Seven calibration star deflections are shown, with elevation angles ranging from 68.3° to 12.1° . A sky brightness deflection is shown for the sky in the Selected Area 111,⁸ which contains calibration stars for the television sensors. Table 2 is a reproduction of the print-out from the computer program. The input data to the program from the photometric deflections of Figure 5 are listed in the output with the exceptions of the sky brightness deflection and the area of coverage of the photometer. The sky brightness deflection was 2mm, and the area of sky covered by the photometer was 2.24×10^5 square arc seconds for this example.

As a graphical check on the extinction calculation, Figure 6 is a

graph of the points $y = m_s + 2.5 \log x_s$ and $x = \sec z_s$, from Equation 3, as calculated for this example. The slope of the graph is the atmospheric extinction coefficient ϵ . From least squares analysis of the spread in the data points, the standard deviation in ϵ is calculated to be $0.01/\text{air mass}$, and in a_0 it is 0.02 .

Assuming a $\pm 10\%$ error in measuring the sky brightness deflections, and a $\pm 5\%$ error in determining the area of sky covered by the photometer, the standard deviation in the sky brightness is 0.1 .

6. Image Stability. Image stability has been measured by four methods at the ETS:

6.1. TV Monitor. On a few occasions, image stability at the ETS has been as poor as 10-15 arc seconds, in which case, point images on a TV monitor of the ETS sensor are observed to increase in diameter. The resolution of the current sensors is limited by the TV cameras to 4 or 5 arc seconds. For example, if the image of a star increases in diameter to 1/8th inch on a TV monitor on which 15 inches on the monitor display corresponds to 0.5° , the angular diameter of the image subtends about 15 arc seconds. Such times when the seeing was poor enough to cause the TV image to increase in diameter beyond 4 to 5 arc seconds were recorded, if it was noticed. This method is useful only if the seeing is worse than 5 arc seconds, which is infrequent.

6.2. Microscopic Observation of a Seeing Disk. In this case, the seeing disk diameter is measured directly by using a filar micrometer microscope which is mounted at the focal plane of the telescope in place of the TV camera. Optical bench tests of the ETS telescopes, employing interferometry and Hartmann tests, indicated that about 80 % of the light

energy from a point source was contained in 0.8 arc sec. Seeing disk measurements were extensively made when the telescopes were installed at the ETS to verify correct optical alignment. Since the TV camera must be removed for these measurements, this method of measuring image stability has been used infrequently since the telescopes were installed. However, the filar micrometer microscope could be mounted on the eyepiece of the telescope, which may operate with the TV camera in place by means of a 45° mirror, if it is later decided that regular image stability measurements are necessary.

6.3. Photographic Plate. When optical alignment of a telescope was completed upon installation, a photographic plate was exposed on a star field to examine the quality of point-source images across the field. A filar micrometer microscope was used to measure diameters of the point-source images on the plate. When the telescope was properly collimated, the measured angular diameter of an unsaturated star image was the average atmospheric seeing disk during the exposure time, which was usually several minutes. Since this method requires the TV camera to be removed and replaced by a plate holder, it has been used only during telescope installation tests.

6.4. Binary Star Separation. Image stability has most recently been measured at the ETS by examining the appearance of certain binary star images. This method is convenient because the observer merely has to look at the stars through the eyepiece of the telescope by putting the 45° mirror in front of the TV camera. From the appearance of the binary star image; i.e., whether the two stars are clearly resolved, just resolved, or not resolved, atmospheric image stability may be deduced from the known separation of the stars.

IV. The Measurements

1. Night-Sky Brightness and Atmospheric Extinction. The range of night-sky brightness values and atmospheric extinction coefficients measured over the 18 month period are shown in Table 3. Also shown in Table 3 is the moon status, and local relative humidity (as measured on our weather instruments) during the measurements. The sky brightness values given are typical measurements of different portions of the sky on the evenings indicated; i.e., the actual sky brightness encountered on a given night of measurement would fall in the indicated range. As an illustration, Table 4 gives the actual night-sky brightness encountered at different positions on the celestial equator on 7 of the evenings.

Figure 7 is a plot of the atmospheric extinction coefficients and relative humidity measurements for the time period, which were taken from Table 3. The wide variation in the atmospheric extinction is indicative of its many factors of dependence. The time period covers two winter seasons, 1975-76 and 1976-77. The ETS experienced considerably less precipitation during its first winter than it did during the second, and the trends of atmospheric extinction and relative humidity measurements during the second winter are seen to be slightly higher.

2. Accuracy of Measurements. It is estimated that the photometric deflections were measured to $\pm 10\%$ accuracy, and the area of sky covered by the photometer was measured to $\pm 5\%$ accuracy. From the least squares analysis, these errors correspond to standard deviations of $0.02/\text{air mass}$ in atmospheric extinction, and $0.1/(\text{arc sec})^2$ in night-sky brightness.

3. The Effect of the Moon on Night-Sky Brightness. The effect of the moon on night-sky brightness was investigated. In Table 4, a gibbous moon was visible on 13 January and a full moon was visible on 12 May 1976. On 12 May 1976, a haze was present over the entire sky due to a vigorous dust storm which occurred during the day and moonlight scattered from the dust made the sky very bright, as indicated in Table 4. Figure 8 is a graph of the sky brightness along the celestial equator on that evening. Atmospheric extinction was not noticeably worse, which may indicate that the dust was close to the ground.

Figure 9 is a graph of night-sky brightness as a function of angular distance from the moon for 3 different lunar phases on the nights indicated. The sky brightness from the full moon as shown for May 12, 1976, is about 1 visual magnitude brighter than that shown for the full moon on September 22, 1976, because of the presence of dust on the former date. It is apparent that sky brightness increases at lower elevations in all cases shown in Figure 9. This is because the photometer sees a greater volume of atmosphere at the lower elevations, and hence a greater intensity of scattered moonlight.

4. The Effects of the Stallion Range Center Night Lights on the Night-Sky Brightness at the GEODSS ETS. Concern has been expressed about a possible effect of the Stallion Range Center night lights on the night-sky brightness at the GEODSS ETS. The Stallion Range Center is located about $\frac{1}{2}$ mile east of the ETS. Consequently, a series of night-sky brightness measurements were taken over the Stallion Range Center on January 29, 1976, with the night lights turned on and off. The measurements were taken over

the azimuthal extent of the center at elevations of 5° , 10° , 20° , and 40° . Since such measurements were cumbersome with the equatorial mount of the ETS sensor for these measurements, the photometer was mounted on an 8-inch Celestron telescope with its mount set up in an alt-azimuth configuration.

Table 5 shows the results of the tests. In addition to the sky brightness measurements over the Stallion Range Center, Table 5 shows like measurements taken over Albuquerque and Belen, New Mexico, where a faint glow was observed near the horizon. It is seen from Table 5 that the night-sky brightness over the Stallion Range Center was not affected by the lights at elevations of 10° to 40° . Also, the sky brightness measurements over Belen and Albuquerque, New Mexico, did not show an appreciable effect due to the city lights.

5. Image Stability Summary. Image stability has seldom been a problem at the ETS because of the relatively coarse resolution (4 or 5 arc seconds) of the ETS sensors. For example, image stability poor enough to seriously affect the TV sensors was noted only on 5 of the nights during the time period when the ETS was operating. Table 6 lists image stability measurements made at the ETS during the time interval which were recorded.

6. Weather Summary. Table 7 presents a summary of cloud cover at and near the ETS. During the time interval, 46% of the nights were clear, i.e., no clouds were observed which affected or would affect satellite observations, 29% of the nights were partly clouded, when limited operation was possible, and 25% of the nights were completely clouded. The most severe cloud cover occurred during the rainy months of July, August, and September.

The survey in Table 7 was taken from visual inspection of the night-sky at the ETS, or when nobody was present at the ETS, from Socorro, New Mexico, in the direction of the ETS. On nights when the ETS was not operating, the sky was only occasionally inspected, and the percentage of cloudless nights may actually be smaller than 46%.

V. Conclusions.

A. The Present Results.

A.1. Atmospheric Extinction. The average atmospheric extinction measured at the GEODSS ETS during the 18 month interval is $0.25 m_v / \text{air mass}$, with slightly higher values occurring primarily during the rainy summer months.

A.2. Night-Sky Brightness. The night-sky brightness measurements at the ETS indicate that the average dark sky, with the moon set, is $21.0 m_v / (\text{arc sec})$, and the average bright sky, with the presence of a full or gibbous moon, is $18.0 m_v / \text{arc sec}$. When the moon is visible, night-sky brightness varies with angular distance from the moon, and from the horizon. Dust, which occasionally is present in the air at the ETS, increases night-sky brightness on moonlit nights, but does not affect atmospheric extinction appreciably.

A.3. Image Stability. On rare occasions, image stability at the ETS has been worse than 4-5 arc seconds, which reduces the detection sensitivity of the present ETS sensors. Only 5 such occasions were recorded during the 18 month interval.

A.4. Weather. The GEODSS ETS can expect to be able to operate on 75% of the nights during the year, and be free of cloud interference on about 46% of the nights.

B. Projects in Progress for Future Measurements.

The following projects are in progress at the ETS which concern astronomical sky conditions:

B.1. The GEODSS operating real-time system is being equipped with a program to point the telescope at a sequence of selected calibration stars for the atmospheric extinction measurement, store the photometric signal, and calculate the atmospheric extinction coefficient, on a real-time basis. Such a program could also determine night-sky brightness on a real-time basis.

B.2. A program is being written to predict the night-sky brightness on moonlit nights near scheduled satellite observations. The program will use as input data the phase of the moon, the angular distance of the satellite from the moon, and the elevation of the satellite from the horizon.

ACKNOWLEDGEMENT

I sincerely thank the GEODSS ETS site personnel of M.I.T., Lincoln Laboratory and the U.S.A.F. Aerospace Defense Command who have helped take the measurements reported herein. In particular, I thank the following personnel of Group 94, M.I.T., Lincoln Laboratory: A. S. Friedman and W. J. Taylor for writing the computer program to calculate atmospheric extinction and night-sky brightness; Dr. J. M. Sorvari for taking several of the extinction measurements as indicated, and the image stability measurements from binary star observations; and Mrs. Coni Johnson for typing the manuscript.

REFERENCES

1. W. A. Baum, "The Detection and Measurement of Faint Astronomical Sources," in Astronomical Techniques, Vol. II, edited by W. A. Hiltner (University of Chicago Press, Chicago, 1962).
2. R. Weber and T. H. Brooks, "The Limits of Detectability of a Low-Light-Level Point-Source Sensor as a Function of Telescope Aperture, Sensor Resolution, Night-Sky Background, and Pre-readout Electron Gain," Technical Note 1974-21, Lincoln Laboratory, M.I.T. (16 August 1974), DDC AD-785137/1.
3. R. Weber, "Visual Magnitude Flux Rate Density Standards for Sunlight Incident on Photoemissive Surfaces," Technical Note 1974-20, Lincoln Laboratory, M.I.T. (6 May 1974), DDC AD-779822/6.
4. L. S. Macknik and K. E. Kissell, "A Study of Sky Brightness and Extinction Effects in Limiting the Baker-Nunn Camera System," ARL TN 71-0086, U.S.A.F. Publication (June 1971).
5. "Photomultiplier Tubes," RCA Electronic Components Div., Harrison, N.J., 07029 (1971).
6. B. Iriarte, H. L. Johnson, R. I. Mitchell, and W. K. Wisniewski, "Five- Color Photometry of Bright Stars," Sky and Telescope **30** (1965).
7. R. H. Hardie, "Photoelectric Reductions," in Astronomical Techniques, Vol. II, edited by W. A. Hiltner (University of Chicago Press, Chicago, 1962).
8. A. U. Landolt, "UBV Photoelectric Sequences in the Celestial Equatorial Selected Areas 92-115," Astron. J. **78**, 959 (1973).

TABLE I
COMPONENTS OF THE TWO PHOTOELECTRIC PHOTOMETERS USED AT THE ETS FOR
NIGHT-SKY BRIGHTNESS AND ATMOSPHERIC EXTINCTION MEASUREMENTS.

Photometer	Time Period Used	Tube	Photocathode	Operating High Voltage	Fore Optics	FOV (Degrees)
1. U.S.A.F Avionics Laboratory Prototype 4 Photometer: Picoammeter, Kiethley 410A; Power Supply, Kiethley 246.	August 1975- August 1976	RCA 4526	RCA-111	-1250	500mm f/8 Catadioptric	0.5
2. Pacific Photometric Instruments: Type 124 Digital Photometer, Type 401 Telescope Coupler, Type 50B PMT housing.	August 1976- Present	EMI 9785B	S-20	-1000	90" f/15 Refractor	0.15 or 0.072

TABLE 2
COMPUTER PRINT-OUT OF ATMOSPHERIC EXTINCTION COEFFICIENT AND
NIGHT-SKY BRIGHTNESS FOR SEPTEMBER 20, 1976.

Star No.	Visual Magnitude	Pen Deflection (mm)	Zenith Distance (Degrees)
1	4.830	6.500	77.900
2	4.520	28.000	27.000
3	5.160	15.000	21.700
4	4.460	30.000	26.800
5	4.700	15.000	68.100
6	4.820	10.000	72.600
7	4.670	20.000	51.800

=>

ATMOSPHERIC EXTINCTION COEFFICIENT: 0.3456
A0 = 0.85103599E+01
SKY BACKGROUND BRIGHTNESS (VISUAL MAG/SQ ARC SEC): 21.2478

Note: The sky brightness value printed out corresponds to a deflection of 1 mm, and not the actual deflection of 2 mm. The sky brightness corresponding to the 2 mm deflection is $20.5/(\text{arc sec})^2$. If several sky brightness readings are taken on a given night, the program is run for a deflection of 1 mm, and the true sky brightness values are calculated from the 1 mm value, to avoid running the program for each sky brightness reading.

TABLE 3
NIGHT-SKY BRIGHTNESS, ATMOSPHERIC EXTINCTION, AND RELATIVE HUMIDITY
MEASUREMENTS TAKEN AT THE GEODSS ETS FROM
AUGUST, 1975 TO MARCH, 1977.

Date of Measurement	Atmospheric Extinction Coefficient m_v /atmosphere	Night-Sky Brightness Range: m_v /(arc sec) ²	Fraction of Moon Disk Visible	Average Relative Humidity (%)
29 Aug 75	0.20	19.8 - 20.2	0.5	-
15 Sep 75	0.32	18.2 - 19.1	0.75	60
16 " "	0.36	18.6 - 19.4	0.75	60
17 " "	0.32	18.5 - 19.3	0.9	60
22 " "	0.34	18.5 - 19.1	1.0	50
23 " "	0.17	18.8 - 19.4	0.9	35
24 " "	0.18	19.2 - 20.8	- -	47
25 " "	0.23	20.1 - 20.7	- -	44
03 Oct "	0.03	20.2 - 20.7	- -	47
06 " "	0.31	19.2 - 20.4	- -	30
07 " "	0.14	19.2 - 20.1	- -	35
08 " "	0.24	19.1 - 20.4	- -	35
09 " "	0.19	19.4 - 20.2	- -	35
23 " "	0.23	18.2 - 18.4	0.75	30
24 " "	0.16	19.1 - 20.4	- -	23
06 Nov "	0.25	20.0 - 20.3	- -	27
10 " "	0.20	19.6 - 20.9	- -	30
14 Dec "	0.28	19.8 - 21.1	- -	47
17 " "	0.18	17.5 - 18.2	0.75	45
30 " "	0.20	20.8 - 22.5	- -	45
06 Jan 76	0.22	20.0 - 20.9	- -	42
07 " "	0.27	20.3 - 20.7	- -	33
08 " "	0.28	20.3 - 21.0	- -	40

Note: Measurements Designated by (*) were taken by Dr. J.M. Sorvari,
Group 94, M.I.T., Lincoln Laboratory.

TABLE 3 (CONTINUED)

Date of Measurement	Atmospheric Extinction Coefficient m_v /atmosphere	Night-Sky Brightness Range: m_v /(arc sec) ²	Fraction of Moon Disk Visible	Average Relative Humidity (%)
13 Jan 76	0.16	17.7 - 18.5	0.75	33
29 " "	0.14	21.3 - 22.6	- -	35
30 " "	0.18	21.4 - 21.8	- -	27
26 Feb "	0.25	20.5 - 21.2	- -	18
28 " "	0.23	20.5 - 21.0	- -	20
09 Mar "	0.18	19.8 - 19.6	0.4	20
19 " "	0.32	18.5 - 18.8	1.0	20
24 " "	0.34	20.7 - 21.2	- -	10
25 " "	0.23	20.5 - 20.9	0.3	20
26 " "	0.19	20.9 - 21.1	- -	15
30 " "	0.21	20.9 - 21.1	- -	30
31 " "	0.23	20.3 - 21.5	- -	20
27 Apr "	0.24	20.3 - 21.5	- -	20
01 May "	0.35	20.7 - 21.1	- -	60
05 " "	0.37	20.2	0.2	80
12 " "	0.23	17.1 - 18.2	0.9	50
15 " "	0.27	16.3 - 18.6	1.0	30
26 " "	0.14	20.8 - 20.6	0.2	50
27 " "	0.22	21.1 - 20.9	- -	33
28 " "	0.26	20.3 - 20.5	- -	18
01 Jun 76	0.25	20.9	- -	15
02 " "	0.28	21.3	- -	20
03 " "	0.33	21.1 - 21.4	- -	35
14 " "	0.19	17.3 - 18.7	1.0	10
15 " "	0.25	17.8 - 19.3	1.0	10
16 " "	0.20	18.8 - 20.3	0.9	15
17 " "	0.23	19.2 - 20.8	0.8	10

TABLE 3 (CONTINUED)

Date of Measurement	Atmospheric Extinction Coefficient m_v /atmosphere	Night-Sky Brightness Range: m_v /(arc sec) ²	Fraction of Moon Disk Visible	Average Relative Humidity (%)
18 Jun 76	0.23	20.9	0.7	20
22 " "	0.25	20.7	0.4	40
23 " "				
28 " "	0.18	20.0 - 21.5	- -	40
01 Jul "	0.53	20.3 - 21.3	- -	50
07 " "	0.18	21.9	- -	45
26 Aug 76	0.35	21.0 - 21.8	- -	50
13 Sep 76	0.26	19.4 - 21.0	0.9	50
16 " "	0.34	20.2	0.7	60
20 " "	0.35	20.5 - 20.6	0.3	60
21 " "	0.32	21.0	- -	65
27 " "	0.27	- - - - -	0.1	50
28 " "	0.26	20.5	0.2	65
* 29 " "	0.22	20.3	0.2	55
04 Oct 76	0.32	18.4 - 20.5	0.75	60
07 " "	0.19	16.4 - 17.9	1.0	55
08 " "	0.21	16.8 - 17.9	1.0	40
* 15 " "	0.30	22.4	0.5	35
* 29 " "	0.24	- - - - -	- -	75
* 01 Nov 76	0.26	- - - - -	- -	75
* 02 " "	0.25	- - - - -	- -	40
* 22 " "	0.32	- - - - -	- -	75
* 20 " "	0.36	- - - - -	- -	35
* 21 " "	0.35	- - - - -	- -	60
* 22 " "	0.33	22.3	0	40
06 Jan 77	0.33	18.3 - 17.4	1.0	75
18 " "	0.27	21.6	0	60

TABLE 3 (CONTINUED)

Date of Measurement	Atmospheric Extinction Coefficient m_V /atmosphere	Night-Sky Brightness Range: m_V /(arc sec) ²	Fraction of Moon Disk Visible	Average Relative Humidity (%)
19 Jan 77	0.56	21.8	0	50
* 24 " "	0.24	- - - - -	- -	65
* 25 " "	0.20	16.5 - 18.6	0.5	55
* 26 " "	0.26	19.3 - 22.5	0.6 Down	55
08 Feb 77	0.24	18.5 - 20.9	0.7	55
13 " "	0.18	21.7	0	55
* 16 " "	0.28	21.6 - 22.1	0	70
* 23 " "	0.31	18.7 - 22.4	0.3 Down	33
* 26 " "	0.41	18.9 - 20.9	0.6	50
* 27 " "	0.27	18.5 - 20.5	0.7	50
* 01 Mar "	0.26	17.0 - 19.7	0.8	35
06 " "	0.30	16.1 - 18.5	1.0	50

TABLE 4
NIGHT SKY BRIGHTNESS READINGS ACROSS CELESTIAL EQUATOR
ON EVENINGS OF INDICATED DATES.

Position on Celestial Equator		Night-Sky Brightness in m_v /atmosphere:						
Local Hour Angle (Hours)	Dec. (Degrees)	10 Nov. 1975	30 Dec. 1975	08 Jan. 1976	13 Jan. 1976 Gibbous Moon	28 Feb., 1976 0430 0930 UT		12 May 1976 Full Moon
-05	0		21.3					17.0
-04	0	19.8	21.3	19.7	18.0	21.1	20.1	17.2
-03	0	20.1	20.8	20.5	18.0	21.1	20.8	17.7
-02	0	20.3	21.8	20.7	Moon	21.1	20.8	17.0
-01	0	20.5	21.8	21.0	17.8	20.5	21.2	16.8
0	0	20.5	22.5	30.7	17.7	20.9	21.2	17.0
1	0	20.7	21.3	20.8	18.0	21.1	21.2	17.3
2	0	20.1	21.3	20.6	18.3	21.4	21.2	17.4
3	0	19.7	21.0	20.7	18.3	21.1	21.4	17.5
4	0	19.5	20.8	19.5	18.3	20.4	21.4	17.5
5	0		20.4	19.2	17.8		21.0	17.1

TABLE 5
RESULTS OF NIGHT SKY BRIGHTNESS MEASUREMENTS TAKEN OVER
THE STALLION RANGE CENTER AND ALBUQUERQUE, NEW MEXICO.

Over the Stallion Range Center (60° to 135° azimuth).		
<u>LIGHTS OFF</u>		<u>LIGHTS ON</u>
Elevation Degrees	Brightness $m_v/(\text{arc sec})^2$	Brightness $m_v/(\text{arc sec})^2$
5	21.3	20.7
10	21.5	21.3
20	21.5	21.5
30	21.5	21.4
40	21.6	21.5

Over Albuquerque and Belen, N.M. (345° to 0° azimuth).

Elevation Degrees	Brightness $m_v/(\text{arc sec})^2$
5	21.1
10	21.2

Error on all measurements: $\pm 0.2 m_v$.

TABLE 6
SUMMARY OF IMAGE STABILITY MEASUREMENTS AT THE GEODSS ETS.

DATE	IMAGE STABILITY (arc seconds)	METHOD OF MEASUREMENT
11 July 1976	1.6	Photographic Plate
01 September 1976	3.3	Photographic Plate
25 March 1977	Occas. 10-15	TV Monitor
13 January 1977	1.8	Microscope
19 January 1977	Occas. 10-15	TV Monitor
20 January 1977	Occas. 10-15	TV Monitor
25 January 1977	2.0	Binary Stars
27 January 1977	2.5	Binary Stars
13 February 1977	Occas. 10-15	TV Monitor
13 March 1977	Occas. 10-15	TV Monitor

TABLE 7
CLOUD COVER AT THE GEODSS ETS FROM AUGUST, 1975 TO MARCH, 1977.

	Clear Nights	Partly Cloudy Nights	Completely Clouded Nights
12-31 Aug. 1975	7	1	12
Sept.	11	6	13
Oct.	29	1	1
Nov.	19	10	1
Dec.	18	5	8
Jan. 1976	17	12	2
Feb.	13	6	10
Mar.	12	13	6
Apr.	11	9	10
May	12	11	8
June	20	7	3
July	6	11	14
Aug.	7	8	16
Sept.	8	13	9
Oct.	11	13	7
Nov.	17	7	6
Dec.	19	6	6
Jan. 1977	9	10	12
Feb.	10	14	4
Mar.	16	11	4

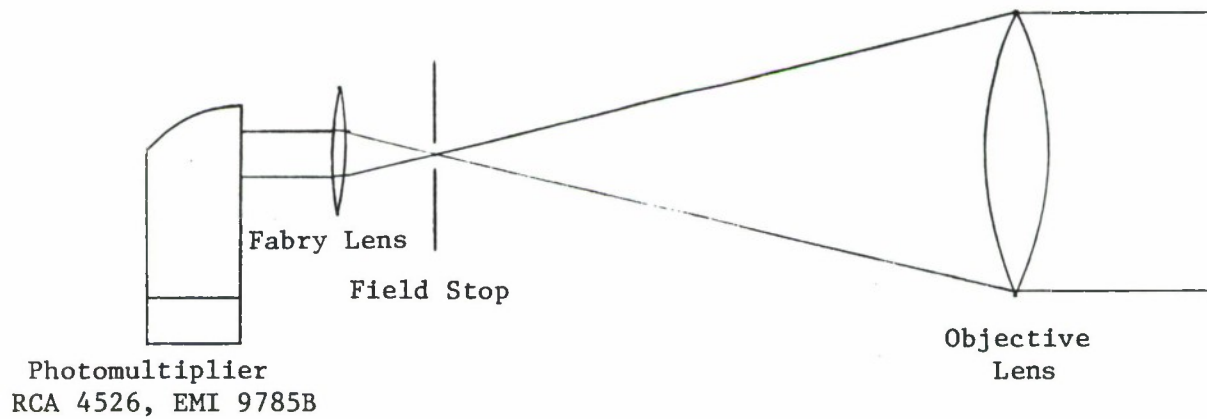


Fig. 1. The optical configuration of the photoelectric photometers used for night-sky brightness and atmospheric extinction measurements.

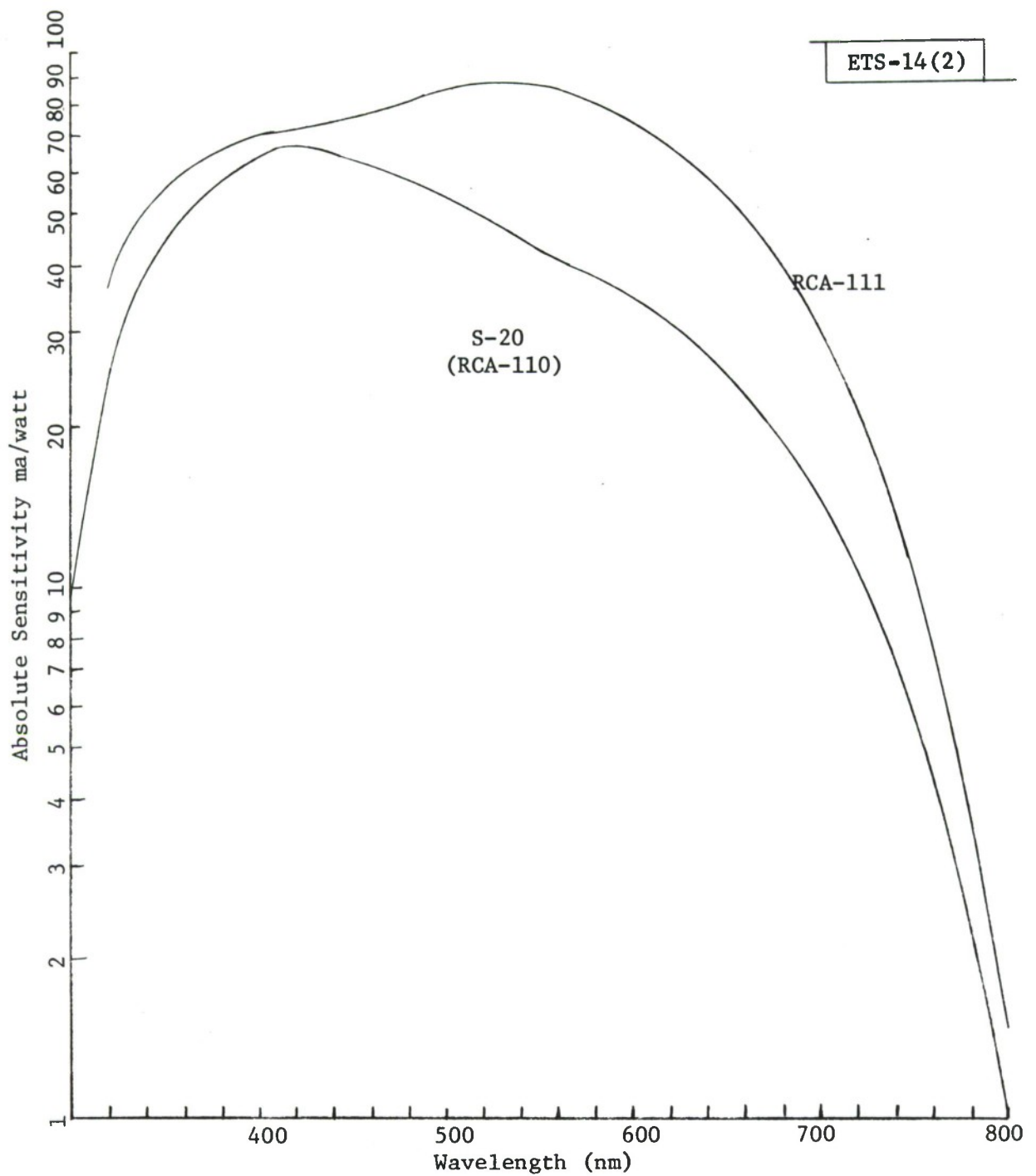


Fig. 2. The spectral response of the S-20 and RCA-111 photocathode, taken from an RCA publication.⁵

Photometer:

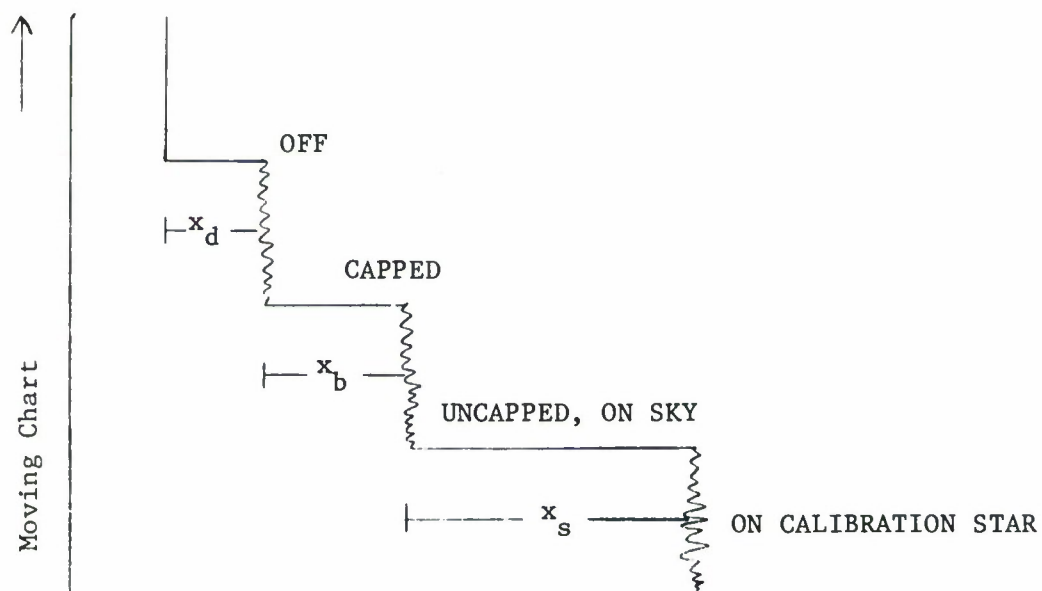


Fig. 3. An illustration of the photometric deflections, x_d , x_b , and x_s .

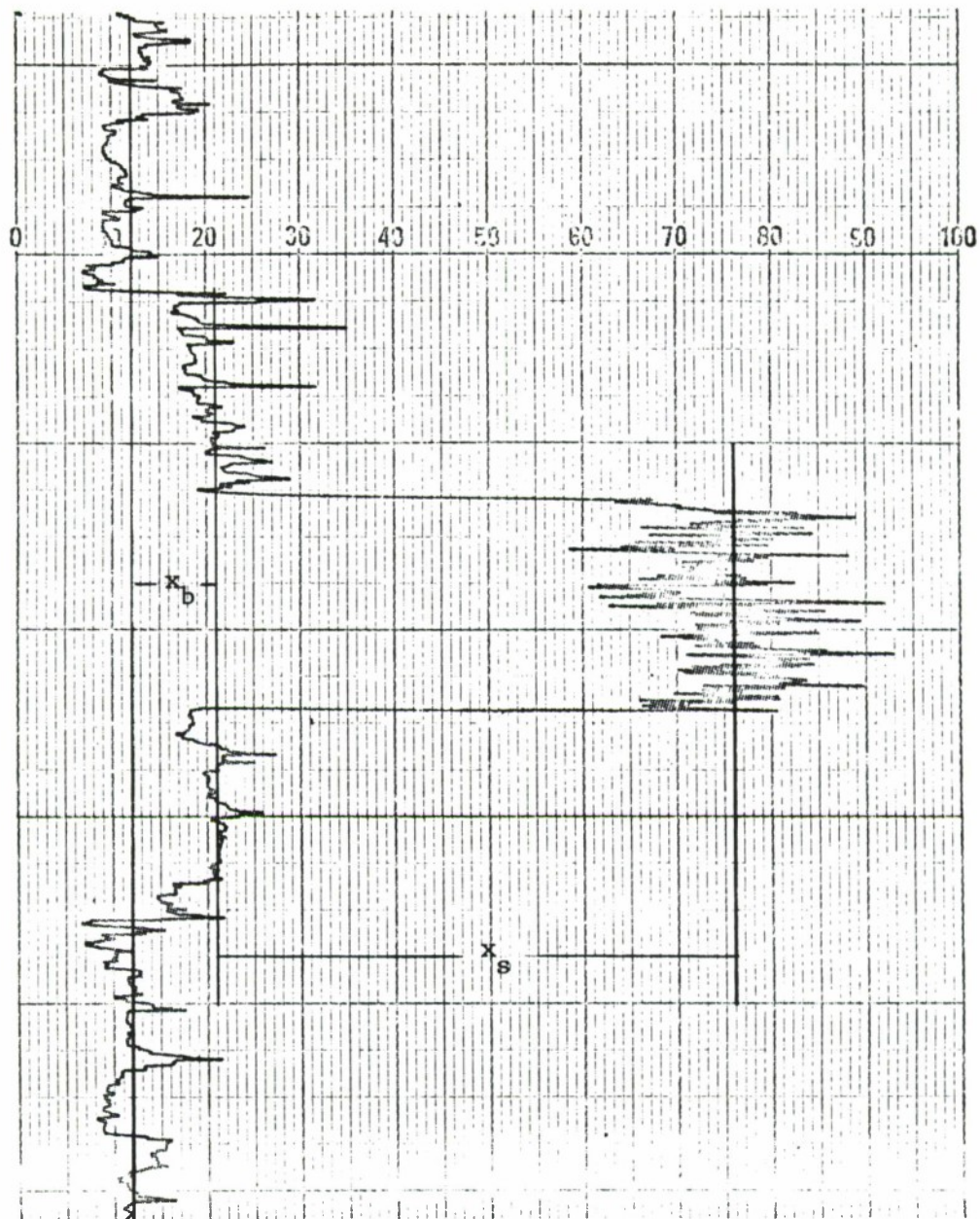
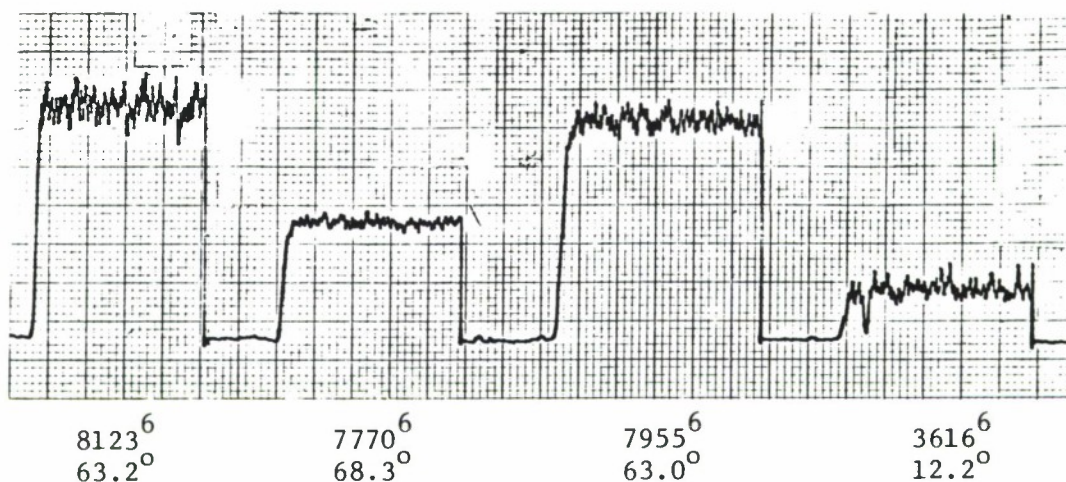


Fig. 4. Reproduction of an actual photometric deflection of the star δ Canis Major at a zenith distance of 61° . The chart shows the sky brightness deflection, and the star deflection as illustrated by Fig. 3.



CAPPED
SA-111
CAPPED

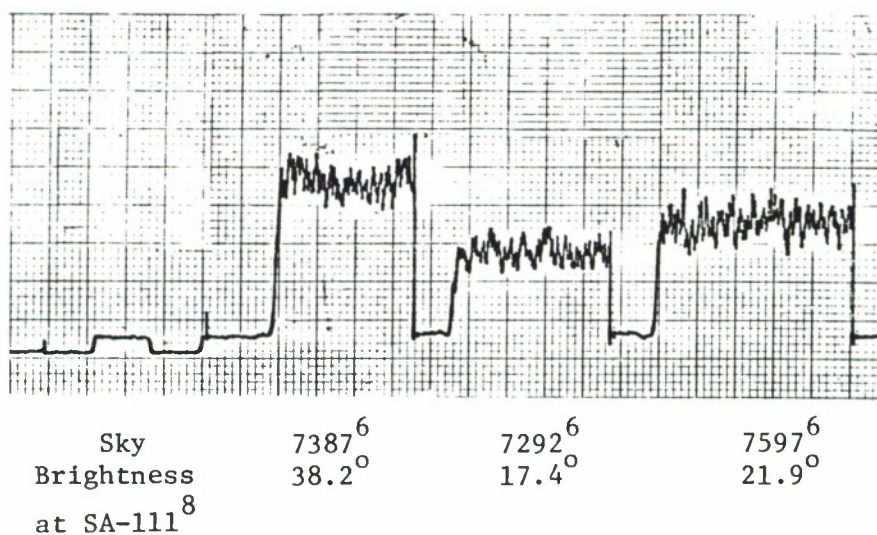


Fig. 5. A reproduction of the photometric reflections from calibration stars and sky brightness taken on September 20, 1976. Stars are indicated by number as referred to in Reference 6, and by elevation.

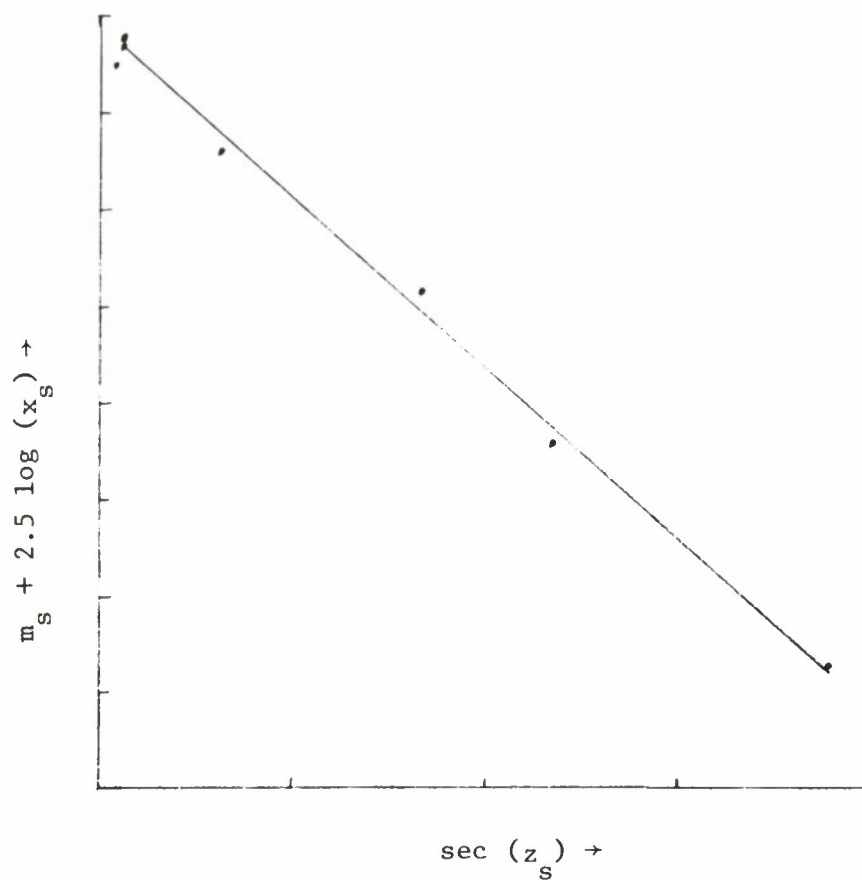


Fig. 6. Atmospheric extinction plot for September 20, 1976. The slope of the straight line fitted to the points, as shown, is the atmospheric extinction coefficient in $m_v/(\text{air mass})$, as indicated by Equation 3 in the text.

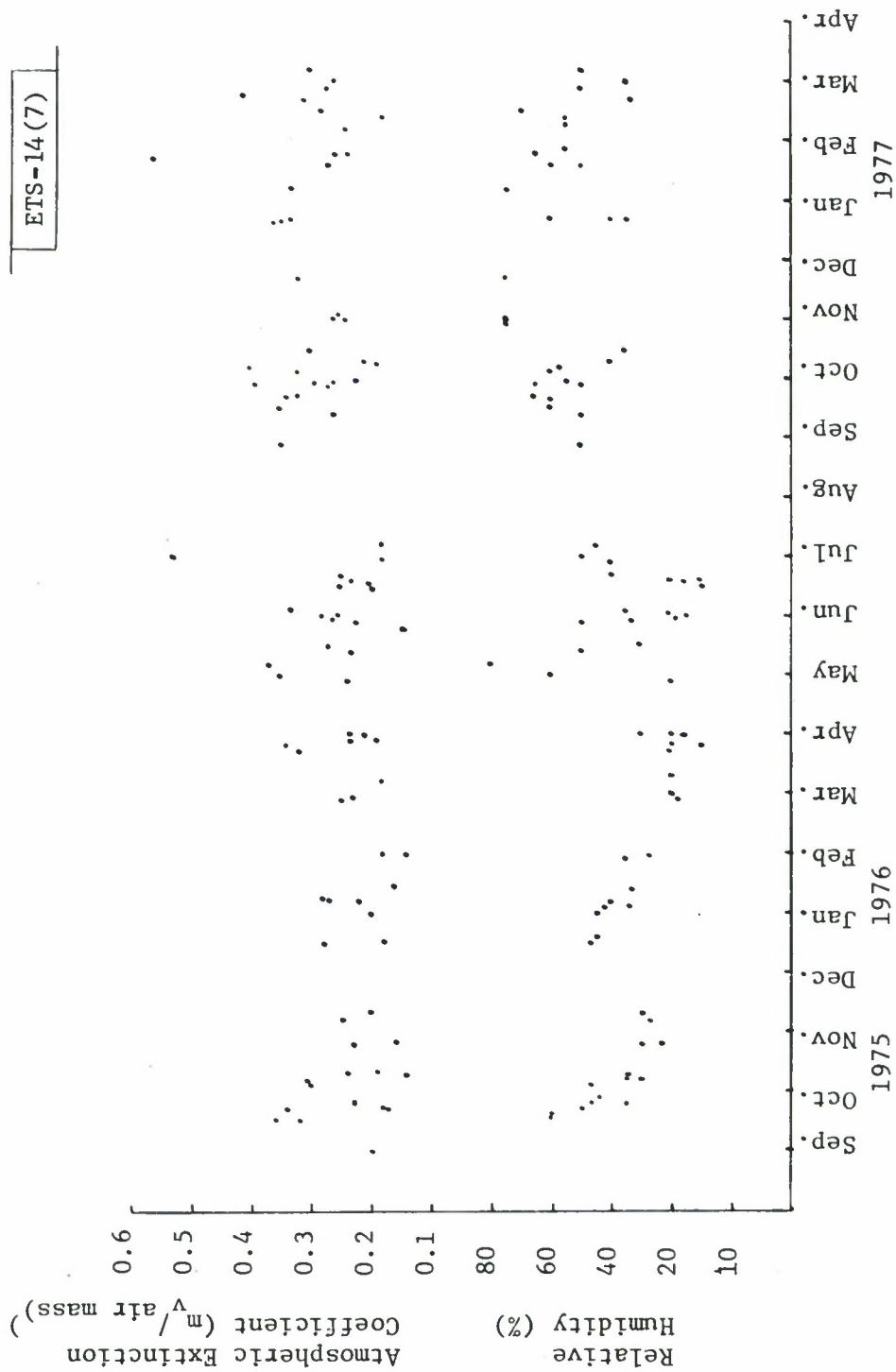


Fig. 7. A condensed plot of atmospheric extinction and corresponding relative humidity taken from Table 3.

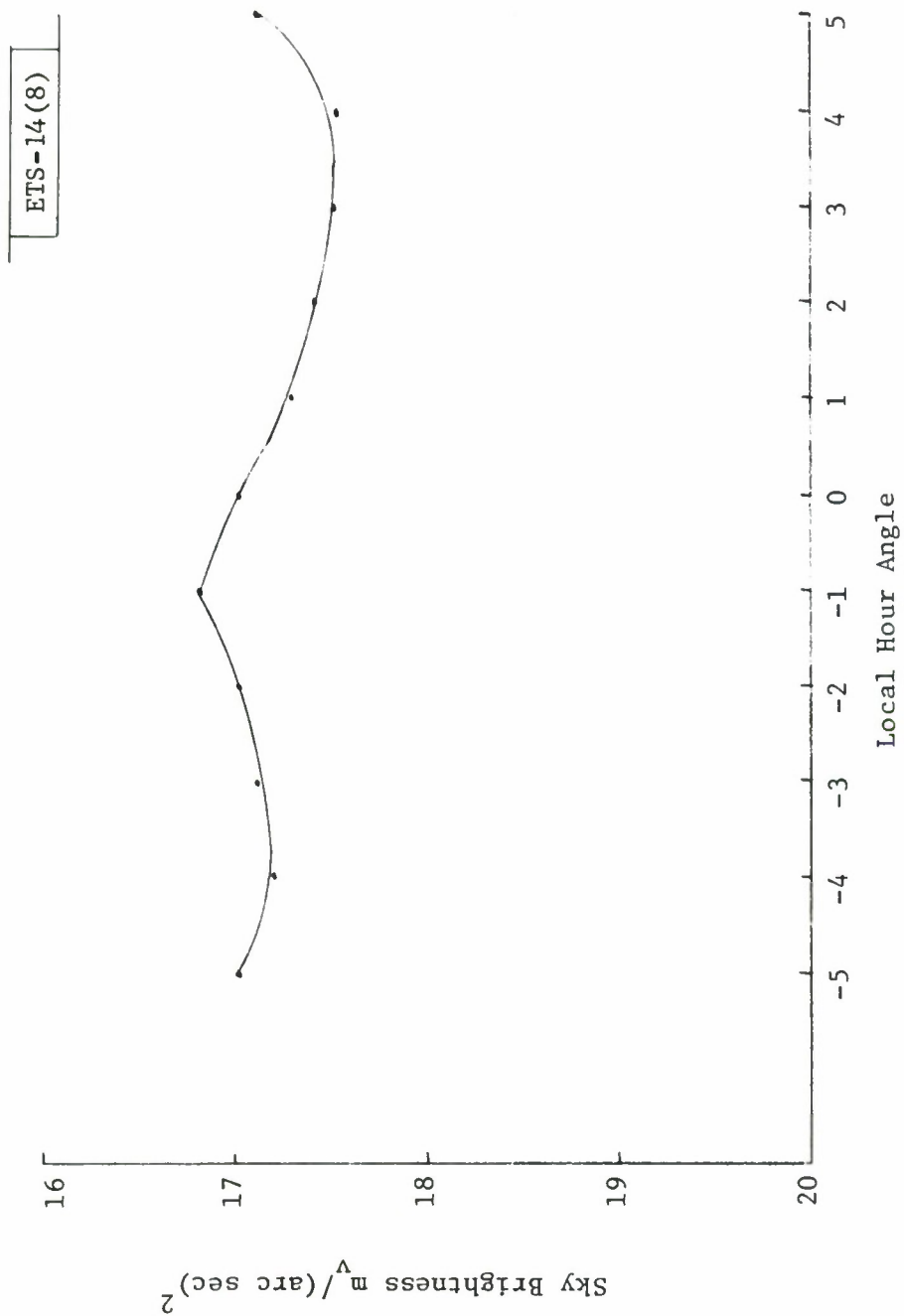


Fig. 8. Night-sky brightness measured along the celestial equator on the night of 12 May 1976.

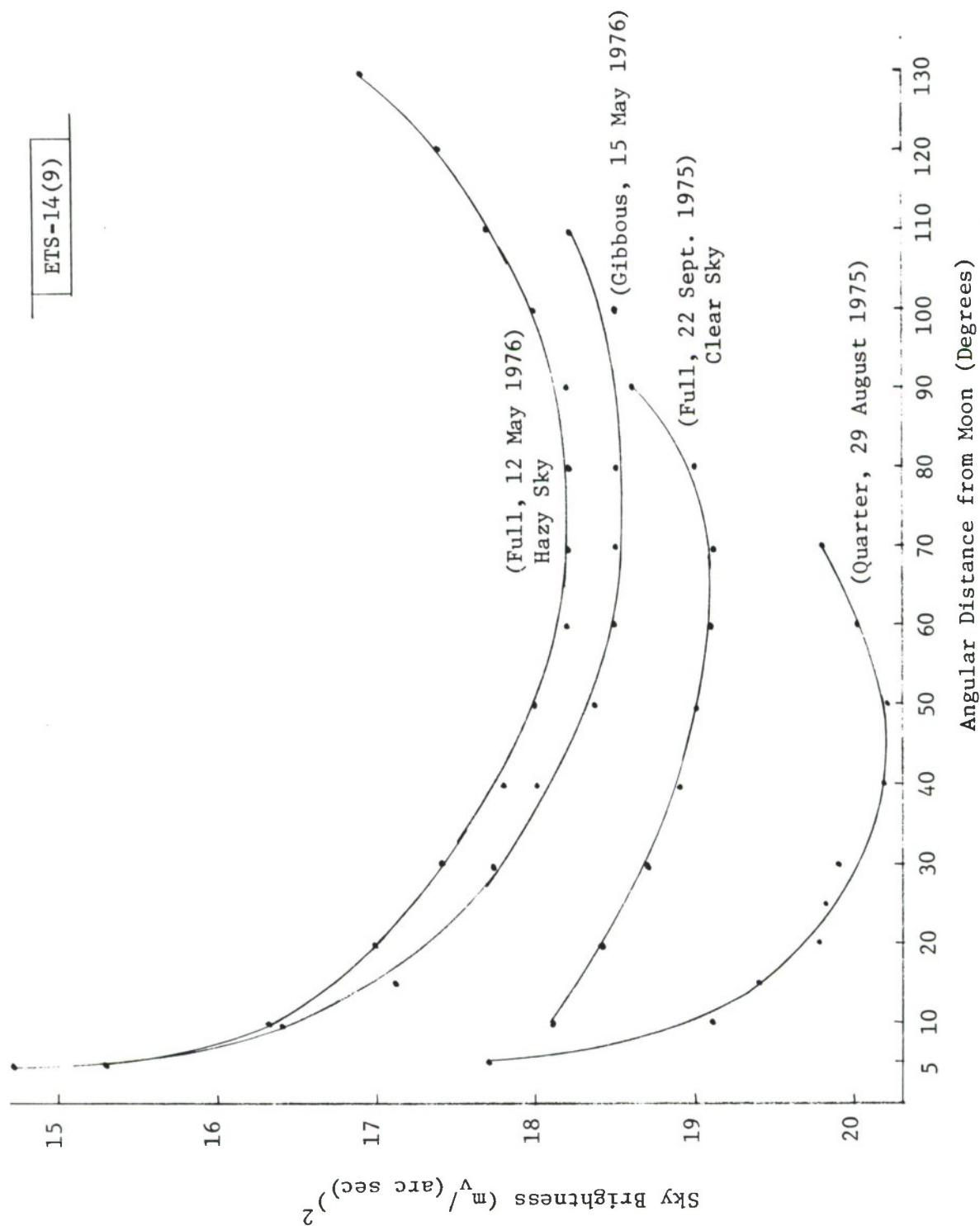


Fig. 9. Night-sky brightness as a function of angular distance from the moon on the dates indicated. The far right points on each graph correspond to an elevation of about 10° from the horizon.

UNCLASSIFIED

SECURITY CLASSIFICATION OF THIS PAGE (When Data Entered)

REPORT DOCUMENTATION PAGE		READ INSTRUCTIONS BEFORE COMPLETING FORM
1. REPORT NUMBER ESD-TR-77-150	2. GOVT ACCESSION NO.	3. RECIPIENT'S CATALOG NUMBER
4. TITLE (and Subtitle) Night-Sky Astronomical Conditions at the GEODSS ETS from August 1975 to March 1977		5. TYPE OF REPORT & PERIOD COVERED Project Report
		6. PERFORMING ORG. REPORT NUMBER Project Report ETS-14
7. AUTHOR(s) Eugene W. Rork		8. CONTRACT OR GRANT NUMBER(s) F19628-76-C-0002
9. PERFORMING ORGANIZATION NAME AND ADDRESS Lincoln Laboratory, M.I.T. P.O. Box 73 Lexington, MA 02173		10. PROGRAM ELEMENT, PROJECT, TASK AREA & WORK UNIT NUMBERS Program Element No. 63428F Project No. 2128
11. CONTROLLING OFFICE NAME AND ADDRESS Air Force Systems Command, USAF Andrews AFB Washington, DC 20331		12. REPORT DATE 21 June 1977
		13. NUMBER OF PAGES 42
14. MONITORING AGENCY NAME & ADDRESS (if different from Controlling Office) Electronic Systems Division Hanscom AFB Bedford, MA 01731		15. SECURITY CLASS. (of this report) Unclassified
		15a. DECLASSIFICATION DOWNGRADING SCHEDULE
16. DISTRIBUTION STATEMENT (of this Report) Approved for public release; distribution unlimited.		
17. DISTRIBUTION STATEMENT (of the abstract entered in Block 20, if different from Report)		
18. SUPPLEMENTARY NOTES None		
19. KEY WORDS (Continue on reverse side if necessary and identify by block number)		
satellite detection GEODSS electro-optics	night-sky brightness atmospheric extinction	image stability cloud cover
20. ABSTRACT (Continue on reverse side if necessary and identify by block number)		
<p>Night-sky brightness, atmospheric extinction, image stability, and cloud cover have been monitored at the GEODSS Experimental Test System, located on the White Sands Missile Range, New Mexico, since August 1975. These quantities have been monitored because the ability of an electro-optical sensor, particularly one which is photon-noise limited, to detect a satellite is a function of them. The results of the measurements of these quantities up through March 1977 are tabulated in this note, accompanied by an explanation of their meaning, and the measurement techniques used.</p>		

UNCLASSIFIED

SECURITY CLASSIFICATION OF THIS PAGE (When Data Entered)